Downregulation of METTL6 mitigates cell progression, migration, invasion and adhesion in hepatocellular carcinoma by inhibiting cell adhesion molecules

AMINA BOLATKAN[1-3], KEN ASADA[2,3], SYUZO KANEKO[2,3], KRUTHI SUVARNA[2-4], NORIKO IKAWA[2], HIDENORI MACHINO[2,3], MASAAKI KOMATSU[2,3], SHUICHIRO SHIINA[1] and RYUJI HAMAMOTO[2,3,5]

[1]Department of Diagnostic Imaging and Interventional Oncology, Graduate School of Medicine, Juntendo University, Tokyo 113-8421; [2]Division of Medical AI Research and Development, National Cancer Center Research Institute, Tokyo 104-0045; [3]Cancer Translational Research Team, RIKEN Center for Advanced Intelligence Project, Tokyo 103-0027, Japan; [4]Department of Biosciences and Bioengineering, Indian Institute of Technology Bombay, Mumbai 400076, India; [5]Department of National Cancer Center Cancer Science, Graduate School of Medical and Dental Sciences, Tokyo Medical and Dental University, Tokyo 113-8510, Japan

Received August 29, 2021; Accepted November 29, 2021

DOI: 10.3892/ijo.2021.5294

Abstract. RNA modifications have attracted increasing interest in recent years because they have been frequently implicated in various human diseases, including cancer, highlighting the importance of dynamic post-transcriptional modifications. Methyltransferase-like 6 (METTL6) is a member of the RNA methyltransferase family that has been identified in many cancers; however, little is known about its specific role or mechanism of action. In the present study, we aimed to study the expression levels and functional role of METTL6 in hepatocellular carcinoma (HCC), and further investigate the relevant pathways. To this end, we systematically conducted bioinformatics analysis of METTL6 in HCC using gene expression data and clinical information from a publicly available dataset. The mRNA expression levels of *METTL6* were significantly upregulated in HCC tumor tissues compared to that in adjacent non-tumor tissues and strongly associated with poorer survival outcomes in patients with HCC. CRISPR/Cas9-mediated knockout of METTL6 in HCC cell lines remarkably inhibited colony formation, cell proliferation, cell migration, cell invasion and cell attachment ability. RNA sequencing analysis demonstrated that knockout of METTL6 significantly suppressed the expression of cell adhesion-related genes. However, chromatin immunoprecipitation sequencing results revealed no significant differences in enhancer activities between cells, which suggests that METTL6 may regulate genes of interest post-transcriptionally. In addition, it was demonstrated for the first time that METTL6 was localized in the cytosol as detected by immunofluorescence analysis, which indicates the plausible location of RNA modification mediated by METTL6. Our findings provide further insight into the function of RNA modifications in cancer and suggest a possible role of METTL6 as a therapeutic target in HCC.

Correspondence to: Dr Ken Asada or Professor Ryuji Hamamoto, Division of Medical AI Research and Development, National Cancer Center Research Institute, 5-1-1 Tsukiji, Chuo-ku, Tokyo 104-0045, Japan
E-mail: ken.asada@riken.jp
E-mail: rhamamot@ncc.go.jp

Key words: hepatocellular carcinoma, HCC, METTL6, RNA modification, tRNA methylation, cell adhesion proteins, epigenetics

Introduction

RNA modifications have emerged as a new layer of epigenetic regulation and are anticipated to further deepen our understanding of molecular complexity and to optimize therapeutic inventions for patients. Currently, more than 170 RNA modifications, including N^6-methyladenosine (m^6A), N^1-methyladenosine (m^1A), and 5-methylcytidine (m^5C), have been identified in nearly all classes of coding and non-coding RNAs (1). Of these modifications, m^6A has been comprehensively characterized; it regulates gene expression and various cellular processes, including RNA folding, stability, splicing, transport, and translation. Accumulating evidence suggests that RNA modifications mediate various biological processes, and aberrant RNA modification has been linked to numerous human diseases such as cancer and cognitive dysfunctions (2-5).

Hepatocellular carcinoma (HCC) is the most common type of primary liver cancer and the fourth leading cause of cancer-related deaths worldwide (6). Similar to the evolution of other cancers, hepatocarcinogenesis is a multistep process involving genetic and epigenetic alterations (7-12). In terms of RNA modulations in HCC, only a few prevalent mRNA regulators have been examined. For example, m^6A writer methyltransferase-like 3 (METTL3) has been reported as an unfavorable prognostic factor in HCC, and its overexpression contributes to HCC progression by reducing cytokine

signaling 2 (SOCS2) messenger RNA (mRNA) stability in an m^6A-dependent manner (13). Intriguingly, METTL3 has been recruited to the transcriptional start sites, and the promoter-bound METTL3 induces co-transcriptionally modified m^6A within the coding region of the transcript (14). Another m^6A writer member, METTL14, is associated with HCC metastasis by regulating the processing of miR-126 (15). Incidentally, miR-126 is downregulated in various cancers and is known to play a role in carcinogenesis in various cancers, including in HCC (16). The m^6A reader protein YTHDF2 has been shown to suppress cancer cell proliferation by destabilizing epidermal growth factor receptor (*EGFR*) mRNA in HCC (17).

To date, only a few studies have been conducted on METTL6, a tRNA methylation enzyme, with limited knowledge about its role and mechanism of action in cancer. One study showed that METTL6 was upregulated in highly proliferative luminal breast cancer (18) and another study revealed that knockout of METTL6 altered cisplatin sensitivity in lung cancer cells (19). Very recently, Ignatova *et al* reported that loss of METTL6 impaired the pluripotency of mouse stem cells, and that this molecular was a vital regulator of HCC cell proliferation (20). Another recently published paper established a prognostic risk score based on five metabolism-related genes, including that of METTL6, indicating high-risk patients had a poor overall survival (OS) compared to low-risk patients with HCC (21).

Although METTL6 has been identified in various human cancers, the characterization of this tRNA modification and its mechanisms of action in cancer remain unclear. Hence, the aim of this study was to investigate the functional roles of METTL6 in cancer development, and to study its potential mechanisms of action. In the present study, we demonstrated that tumorigenicity in HCC was due to the upregulation of METTL6. Furthermore, the depletion of METTL6 mitigated HCC cell proliferation, migration, invasion, and attachment ability, possibly through the regulation of cell adhesion-related genes post-transcriptionally. In addition, METTL6 was found to be localized in the cytosol. Our findings may provide insights into the functional roles of tRNA and post-transcriptional regulation in cancer, and may lead to the development of a therapeutic strategy for HCC.

Materials and methods

Bioinformatics analysis. We retrieved multi-omics data from RNA-sequencing (RNA-seq), DNA promoter methylation, DNA copy number, and clinical information from The Cancer Genome Atlas (TCGA) using cBioPortal (https://www.cbioportal.org) corresponding to a total of 372 HCC samples. The differential expression analysis between HCC and non-HCC tissues and across four different tumor stages, as well as OS and disease-free survival (DFS) analyses were performed using the Gene Expression Profiling Interactive Analysis (GEPIA) webserver (http://gepia.cancer-pku.cn/). In addition, GraphPad Prism 8 software (GraphPad Software, Inc.) was used to analyze the association between DNA copy number alterations (CNAs) and mRNA expression. A one-way ANOVA test was performed to compare mRNA expression levels between groups of different CNAs. Statistical significance was set at $P<0.05$.

Plasmid DNA constructs. The lentiviral packaging plasmids pMD2.G and psPAX2 were obtained from Addgene (#12259 and #12260, Addgene, USA, respectively). To generate inducible Cas9 nuclease-expressing cell lines, we purchased the Edit-R inducible lentiviral plasmid (#CAS11229, Dharmacon, UK). Five individual sgRNAs targeting the *METTL6* gene used in this study were as follows (5'→3' orientation): sgRNA1: 5'-GGAGCTAAGATCATGTAGAG-3', sgRNA2: 5'-ATATGATACAGAAAGATGCA-3', sgRNA3: 5'-GTTTCATAGGTATTAAAACC-3', sgRNA4: 5'-ATAACAACATCCACAGACTC-3' and sgRNA5: 5'-ACAGCAGAAATTGGAACAAG-3'. sgRNAs were designed and cloned into the pLKO.1-puro U6 sgRNA BfuAI large stuffer plasmid (#52628, Addgene). All plasmids were verified using Sanger sequencing.

Cell lines and culture conditions. The human HCC cell lines SNU-423 and SNU-475 were purchased from the American Type Culture Collection (ATCC), and tested and authenticated using DNA profiling for polymorphic short tandem repeat (STR) markers analyzed by BEX Co. Ltd. using GenePrint 10 systems (Promega Corp.) before starting the project (Table SI). The human liver cancer cell lines HepG2, Huh-7, and Li-7 were purchased from RIKEN Bioresource Research Center (RIKEN BRC, Japan), and tested and authenticated using DNA profiling for polymorphic short tandem repeat (STR) markers analyzed by Applied Biosystems using GeneMapper ID software before starting the project (Table SI). SNU-423, SNU-475, Huh-7, and Li-7 cells were cultured as monolayers in RPMI-1640 supplemented with 10% FBS and antibiotics, and HepG2 cells were cultured as monolayers in MEM supplemented with 10% FBS, 0.1 mM NEAA and antibiotics. All cells were maintained at 37˚C in humid air with 5% CO_2. In the present study, SNU423 and SNU475 cells were mainly used as HCC cell lines for various experiments. The reason for this is as follows. i) HepG2 was originally considered a hepatocellular carcinoma cell line, but it has been shown to be a hepatoblastoma (22). In addition, HepG2 cells were established from a younger boy (15 years of age). Therefore, we decided not to use this line in further studies. ii) As for Huh-7 cells, previous literature has indicated that Huh-7 cells may produce adhesion-related factors and growth factors autonomously (23). Therefore, we considered Huh-7 cells as inappropriate because we examined the role of adhesion-related genes with and without METTL6 expression. iii) Regarding Li-7 cells, a previous study showed that of five hepatocellular carcinoma cells, only Li-7 cells showed a population change after two months of culture (24). Then, we decided not to use this line in further studies. iv) SNU-423 is an adult hepatocellular carcinoma that was generated from a 40-year-old man. SNU-475 is another adult hepatocellular carcinoma cell line generated from a 43-year-old man. In addition, we previously constructed a knockout system for both SNU-423 and SNU475 cells using CRISPR/Cas9, and confirmed that the target genes were properly knocked out (25). Hence, we decided to use these two cell lines mainly in this study.

CRISPR/Cas9 gene editing system. A lentivirus transduction system was used to generate CRISPR/Cas9 knockout cells. To produce lentiviruses, viral vectors and

packaging plasmids were co-transfected into 293T cells using Lipofectamine 3000 (#L3000-008, Thermo Fisher Scientific, Inc.) according to the manufacturer's instructions. After 48 h, the cell culture medium containing lentiviruses was collected and filtered through a 0.45-μm filter. Target cell lines were plated in 6-well plates and cultured with lentivirus-containing medium for 3 days, which was carried out in the absence of polybrene. Stable cell clones were selected using blasticidin S (10 μg/ml) (#029-18701, FUJIFILM Wako Pure Chemical Corporation, Japan). For inducible CRISPR/Cas9 knockout experiments, conditional Cas9 expression cells further underwent lentivirus transduction of conditional sgRNA expression plasmid and selection in the presence of both blasticidin S (10 μg/ml) and puromycin (2 μg/ml) (#ant-pr-1, InvivoGen). Knockout of METTL6 was induced by adding doxycycline (Dox) (1 μg/ml) (#D9891, Sigma-Aldrich; Merck KGaA) for 48 h.

Western blot analysis. SNU-423 and SNU-475 cells were lysed with CelLytic™ Reagent (#C2978, Sigma-Aldrich; Merck KGaA) using standard methods. Protein lysates (15 μg) were separated on a 10% SDS-PAGE gel and transferred to nitrocellulose membranes. The membranes were blocked with 5% skimmed non-fat milk for 2 h at 25˚C, and then the membranes were incubated with rabbit polyclonal anti-METTL6 primary antibody (#HPA035166, Sigma-Aldrich; Merck KGaA; dilution used in WB: 1:2,000); rabbit polyclonal anti-METTL2 primary antibody (#PA5-113304, Invitrogen/Thermo Fisher Scientific, Inc.; dilution used in WB: 1:2,000); rabbit polyclonal anti-METTL8 primary antibody (#ab122273, Abcam; dilution used in WB: 1:2,000); rabbit polyclonal anti-ITGA1 primary antibody (#22146-1-AP, Proteintech; dilution used in WB: 1:2,000); chicken polyclonal anti-SPON1 primary antibody (#ab14271, Abcam; dilution used in WB: 1:1,000); goat polyclonal anti-CLDN14 primary antibody (#ab19035, Abcam; dilution used in WB: 1:1,000); and mouse monoclonal anti-α-tubulin (DM1A, EMD Millipore; dilution used in WB: 1:1,000) antibodies at 4˚C overnight. After primary antibody incubation, the membranes were incubated with an HRP-linked donkey anti-rabbit secondary antibody (#NA934V, GE Healthcare, USA; dilution used in WB: 1:5,000) and mouse anti-goat IgG-HRP (#sc-2354, Santa Cruz Biotechnology, Inc.; dilution used in WB: 1:5,000) at 25˚C for 1 h. The signal was detected using the ECL system (#RPN2236, GE Healthcare, USA), and NIH ImageJ software (version 1.53) (National Institutes of Health) was used for quantification (26).

Colony formation assay. Cells were seeded in 6-well plates at a density of 1,000 cells/well and cultured at 37˚C. The culture medium with or without Dox was replaced every 3 days. After 14 days, cells were fixed with 1% formaldehyde (#252549, Sigma-Aldrich; Merck KGaA) and 1% methanol (#137-01823, FUJIFILM Wako Pure Chemical Corporation), stained with 0.05% crystal violet (#V5265, Sigma-Aldrich; Merck KGaA) for 20 min, and then washed three times with Milli-Q water. Colony numbers were quantified using the NIH ImageJ software (26).

Cell proliferation assay. Cell viability was measured using the Cell Counting Kit-8 (CCK-8) (#343-07623, Dojindo Laboratory, Japan). Cells were seeded in 96-well plates at a density of $1.0x10^3$ cells/well and cultured for 24, 48, 72 and 96 h. Then, 10 μl of CCK-8 solution was added and the plates were incubated at 37˚C for 2 h. The absorbance of each well was measured at 450 nm using a microplate reader (Multiskan FC, Thermo Fisher Scientific, Inc.).

Cell scratch assay. Cells were seeded in 6-well plates at a density of $3x10^5$ cells/well and incubated for 24 h. When the cellular confluence reached 90%, a 200-μl pipette tip was used to create wounds in the monolayer cells. The wells were then rinsed with PBS three times to remove any detached cells, and fresh serum-free medium was added. The wells were then placed in an incubator, and visualized using a phase-contrast microscope (Olympus CKX53, Japan) at 0 and 48 h. The percentage of wound area was calculated using the ImageJ software.

Cell invasion assay. For the cell invasion assay, a 96-well Boyden chamber coated with basement membrane extract (BME) was used (#ab235697, Abcam). Prior to the assay, the cells were starved for 24 h in serum-free media. Then, cells were suspended in serum-free medium and seeded into the upper chamber (8.0-μm pore size) at a density of 50,000 cells per well. Further, 200 μl of RPMI medium containing 10% serum was added to the lower chamber. The cells were allowed to invade for 24 h at 37˚C. A standard curve was constructed for each cell type. After incubation, cells were washed carefully, and those that did not invade the lower side of the chamber were removed from the top side. Then, 100 μl of the cell invasion dye and cell dissociation solution were added to each well in the lower chamber. The chamber was incubated at 37˚C for 1 h, and the bottom wells were read at excitation and emission wavelengths of 530/590 nm using a Synergy H1 Hybrid Multi-Mode Reader (BioTrek).

Cell adhesion assay. Cells were seeded in 6-well plates at a density of $0.5x10^5$ cells/well (SNU-423) and $1.0x10^5$ cells/well (SNU-475). The cells were then incubated for 15, 30, 45, and 60 min. Next, the wells were washed with PBS three times to remove any detached cells, and images were obtained using a phase-contrast microscope (Olympus CKX53, Japan) at 15, 30, 45, and 60 min. Cell numbers were calculated using ImageJ software.

RNA-seq and data analysis. Total RNA was extracted using the QIAzol lysis reagent (#79306, Qiagen). Extracted RNA was treated with DNase I (#043-31261, FUJIFILM Wako Pure Chemical Corporation) at 37˚C for 30 min, followed by acid phenol:chloroform extraction (#AM9722, Thermo Fisher Scientific, Inc.). Purified RNA was re-suspended in Takara's buffer for mRNA amplification using 5' template switching PCR with Takara's SMART-Seq v4 Ultra Low Input RNA Kit (both from Takara). The amplified cDNA was fragmented and appended with dual-indexed barcodes using Illumina Nextera XT DNA Library Prep Kits (Illumina, Inc.). Libraries were validated by electrophoresis, pooled, and sequenced on an Illumina NovaSeq 6000 (150 base pairs, paired ends) (Illumina, Inc.). RNA-seq data were mapped to the hg38 version of the human genome using the DRAGEN Bio-IT Platform (v3.6.3)

(Illumina, Inc.). Raw counts were converted into transcripts per million reads. Genes with $q \leq 0.05$ and $|\log2\_ratio| \geq 1$ were identified as differentially expressed genes (DEGs) after the knockout of METTL6 in SNU-423_KO2, SNU-423_KO5, SNU-475_KO3, and SNU-475_KO4. Gene ontology (GO) and Kyoto Encyclopedia of Genes and Genomes (KEGG) enrichment analyses of the DEGs were performed using Metascape (27) with $P<0.05$, indicating statistically significant enrichment. Reads from all sequencing experiments were deposited into the DNA Data Bank of Japan (DDBJ) with the accession number DRA012940.

Chromatin immunoprecipitation sequencing and data analysis. Chromatin immunoprecipitation sequencing (ChIP-seq) analyses were performed using the SimpleChIP Enzymatic Chromatin IP Kit (#9003, Cell Signaling Technology, Inc.) with minor modifications. Briefly, cells cultured in 10 cm^2 dishes were fixed in 1% formaldehyde for 10 min, and fixation was quenched with the addition of glycine to 125 mM for an additional 5 min. Cells were harvested by scraping from the plates and stored at -80˚C. During the solubilization of chromatin, fixed nuclei were sonicated with an E220 focused ultrasonicator (Covaris, USA). Immunoprecipitation antibodies were rabbit polyclonal anti-H3K27ac (#ab4729, Abcam) and rabbit polyclonal anti-CTCF (#3418s, Cell Signaling Technology, Inc.). Approximately 5 μg of chromatin was incubated with the indicated antibody overnight at 4˚C on a rotator. Then, FG Beads HM Protein G (#TAB8848N3173, Tamagawa Seiki, Japan) was added to the solution and washed with buffer, as described previously (28). Immunoprecipitated chromatin was eluted and reverse-crosslinked according to the manufacturer's instructions (#9003, Cell Signaling Technology, Inc.). Immunoprecipitated DNA was purified using a QIAquick PCR Purification Kit (#28106, Qiagen). DNA libraries were prepared using the QIAseq Ultralow Input Library Kit (#180492, Qiagen) for Illumina. Library quality was checked using a TapeStation 4200 instrument (Agilent Technologies, Inc.). DNA libraries were sequenced using the NovaSeq 6000 system (Illumina). Sequencing reads from ChIP-seq experiments were mapped to the hg38 version of the human genome using Bowtie (v2.2.9) and parameters (local) (29). Duplicate reads were removed using the Samtools (v1.3.1). The normalized ChIP-seq signals were visualized using the Integrative Genomics Viewer (IGV; v2.3.91) (30). Reads from all sequencing experiments were deposited into the DNA Data Bank of Japan (DDBJ) with the accession number DRA012940.

Immunofluorescence analysis. Cells were seeded at a density of $1x10^4$ cells/well (SNU-423_KO2) with and without Dox treatment in 2-well chamber culture slides (#154852, Lab-Tek™ II CC2™ Chamber Slide System, Thermo Fisher Scientific, Inc.). After 4 days, the cells were rinsed with ice-cold PBS and fixed with 4% paraformaldehyde (#163-20145, Paraformaldehyde Phosphate Buffer Solution, FUJIFILM Wako Pure Chemical Corporation) for 15 min at 25˚C. Cells were then blocked with 3% BSA (#A-9647, bovine serum albumin, Sigma-Aldrich; Merck KGaA) and 0.3% Triton X-100 [#160-24751, Polyoxyethylene(10) Octylphenyl Ether, FUJIFILM Wako Pure Chemical Corporation] for 60 min. The cells were subjected to immunofluorescence staining with rabbit polyclonal METTL6 primary antibody (#HPA035166, Sigma-Aldrich; Merck KGaA; dilution used: 1:200) overnight at 4˚C. Next, the cells were washed with cold PBS three times for 5 min each time, and incubated with donkey anti-rabbit IgG (H+L) secondary antibody Alexa Fluor 594 (#A21207, Thermo Fisher Scientific, Inc., dilution used: 1:500) at 25˚C for 1 h. The cells were washed with cold PBS and mounted using mounting medium containing DAPI (#H-1200, Vector Laboratories). The cells were examined using fluorescence microscopy (Celldiscover 7, ZEISS) at 20x with 5x5 tiling.

Statistical analysis. Statistical analyses were performed using GraphPad Prism 8.0 (GraphPad Software, Inc.). The cut-off value for *METTL6* mRNA expression was determined at the median level. Differences in *METTL6* mRNA expression levels between HCC samples and control tissues, as well as expression levels at different stages, were calculated using one-way analysis of variance (ANOVA). Survival curves were obtained using Kaplan-Meier curves and log-rank tests. The association of *METTL6* mRNA expression levels with DNA CNAs was assessed using one-way ANOVA. All quantitative results, including relative expression analysis by western blot analysis, cell colony assay, cell proliferation assay, cell scratch assay, and cell attachment assay, are presented as means ± standard deviation (SD) of at least three separate experiments. A two-tailed unpaired t-test was used to compare the mean values between the two groups. Results were considered significant when the P-value was $^{*}P<0.05$, $^{**}P<0.01$, $^{***}P<0.001$, $^{****}P<0.0001$, or NS=non-significant (as indicated with these symbols/initials in the figures).

Results

METTL6 is elevated in HCC tissues and is associated with poor prognosis. First, we established a list of 60 known RNA regulators, including methyltransferases, demethylases, and acetyltransferases. We then analyzed their mRNA expression levels in HCC tumor samples and adjacent non-tumor tissues and examined whether they might be correlated with HCC patient survival rates based on the Cancer Genome Atlas (TCGA) and Genotype-Tissue Expression (GTEx) (31) and OncoLnc platforms based on TCGA independently (32). To assess the novelty of these regulators, we conducted a literature survey of HCC-related studies for each candidate (Table SII and Fig. S1). Notably, these results suggest that METTL6, which was recently identified as a methylcytidine (m^3C) methyltransferase on tRNA (33) might be a promising novel target among all candidates. mRNA expression of *METTL6* was significantly upregulated in HCC tumor tissues compared to that in adjacent non-tumor tissues (Fig. 1A). Meanwhile, a gradual increase in the mRNA level of *METTL6* was observed from tumor stages I to III, while a slight decrease was observed in stage IV (Fig. 1B). This suggests that METTL6 is highly expressed in the early stages of cancer and involved in the development of cancer, and that there is no significant correlation with the degree of cancer progression. Kaplan-Meier analysis revealed that patients with higher *METTL6* expression levels had significantly poorer OS and DFS (Fig. 1C and D), suggesting that *METTL6* could be a potential prognostic indicator for patients

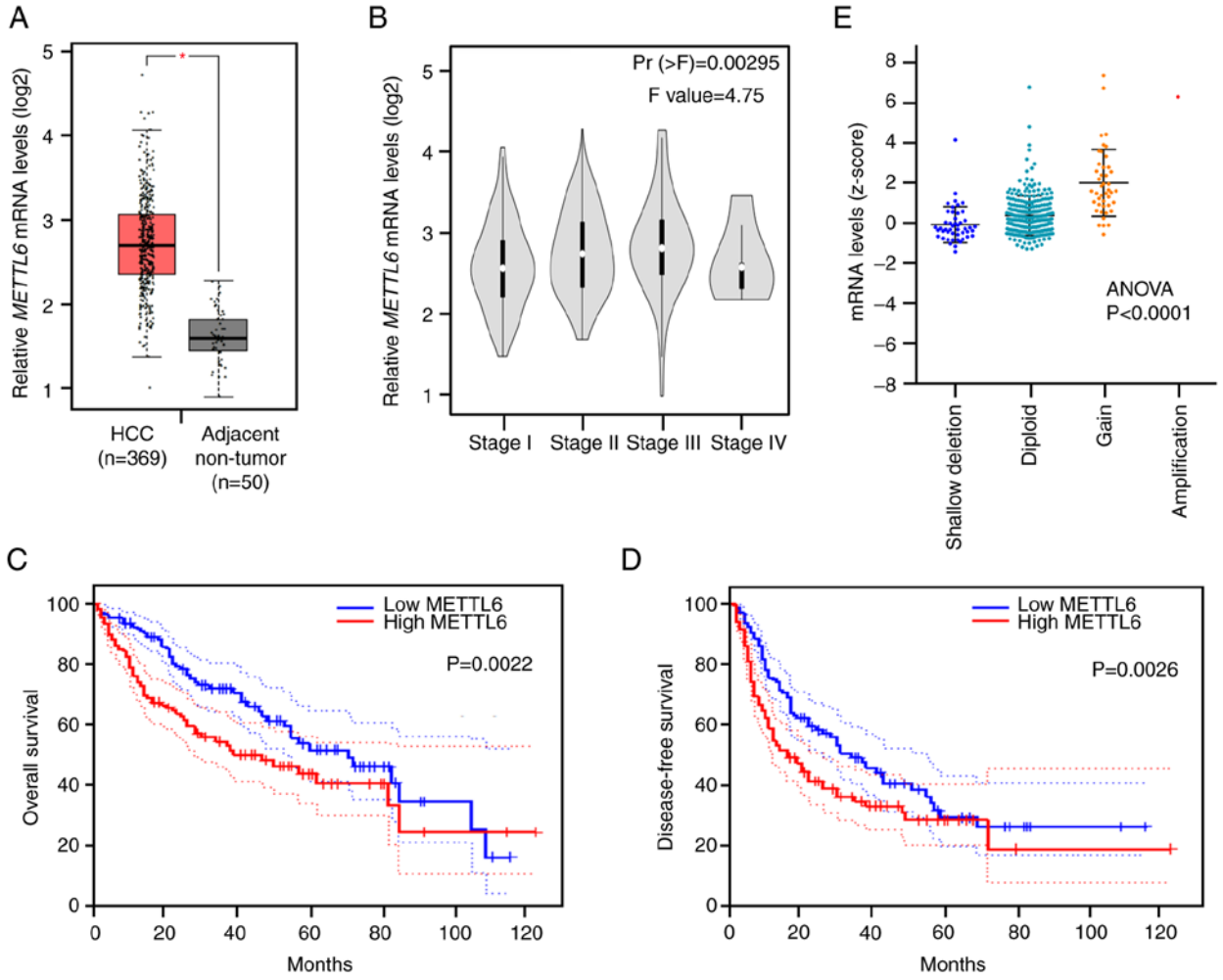

Figure 1. Bioinformatics analysis of METTL6 expression in HCC samples using GEPIA. (A) *METTL6* mRNA expression levels in TCGA_LIHC tumor tissues (n=369) and paired TCGA non-tumor tissues (n=50) using GEPIA. (B) *METTL6* mRNA expression in different stages of HCC (F value=4.75; Pr [>F]=0.00295). (C) Overall survival rate and (D) disease-free survival rate in patients with HCC with high and low *METTL6* mRNA levels. The group cut-off value is based on the median. (E) *METTL6* copy number alterations (CNAs) and *METTL6* mRNA levels (P<1.0e-04, ANOVA test). All data are presented as means±standard deviation. *P<0.05. METTL6, methyltransferase-like 6; GEPIA, Gene Expression Profiling Interactive Analysis; HCC, hepatocellular carcinoma; TCGA, The Cancer Genome Atlas.

with HCC. In addition, we analyzed the TCGA_LIHC (liver HCC) dataset, which contains CNAs and DNA methylation levels of *METTL6*. The *METTL6* copy number was positively correlated with its mRNA levels (Fig. 1E), indicating that the CNAs of *METTL6* might be involved in HCC through alterations in *METTL6* gene expression levels.

Knockout of METTL6 inhibits HCC colony formation, cell proliferation, and cell migration in vitro. To investigate the biological functions of METTL6 in HCC and to assess the effect of METTL6 expression, we first assessed its protein expression levels across five different HCC cell lines (Fig. S2A). We established stable *METTL6* knockout models in SNU-423 and SNU-475 cells using the CRISPR/Cas9 gene editing system, with four independent single-guided RNAs targeting the promoter regions of *METTL6*. Knockout of METTL6 was confirmed using western blot analysis (Fig. 2A). No noticeable changes were observed in the protein expression levels of METTL2 and METTL8, which are the other m^3C methyltransferases that exhibit a functional similarity and are closely related to METTL6, as analyzed by a family tree diagram (33,34). Our bioinformatics analysis indicated that *METTL6* was associated with prognosis; therefore, we first performed multiple cancer phenotypic assays using established knockout cell lines. A colony formation assay was performed to detect the effect of METTL6 expression on the clonogenicity of HCC cells. As anticipated, the METTL6 knockout group had significantly fewer and smaller colonies than the METTL6 expressing groups in both SNU-423 and SNU-475 cell lines, indicating that METTL6 expressing cells had the ability to form colonies (Fig. 2B).

Next, the role of METTL6 in HCC cells was analyzed using the CCK-8 to examine cell proliferation. We found that knockout of METTL6 remarkably inhibited HCC cell viability, suggesting that METTL6 played a role in cell survival (Fig. 2C). Additionally, we investigated the effect of METTL6 knockout on HCC cell migration. Cell scratch assays showed that HCC cell migration was significantly suppressed at 48 h post-scratch in the METTL6 knockout cells (Fig. 3). Collectively, these results indicate that specific tRNA modifications regulated by METTL6 enhance HCC cell colony formation, proliferation, and migration abilities.

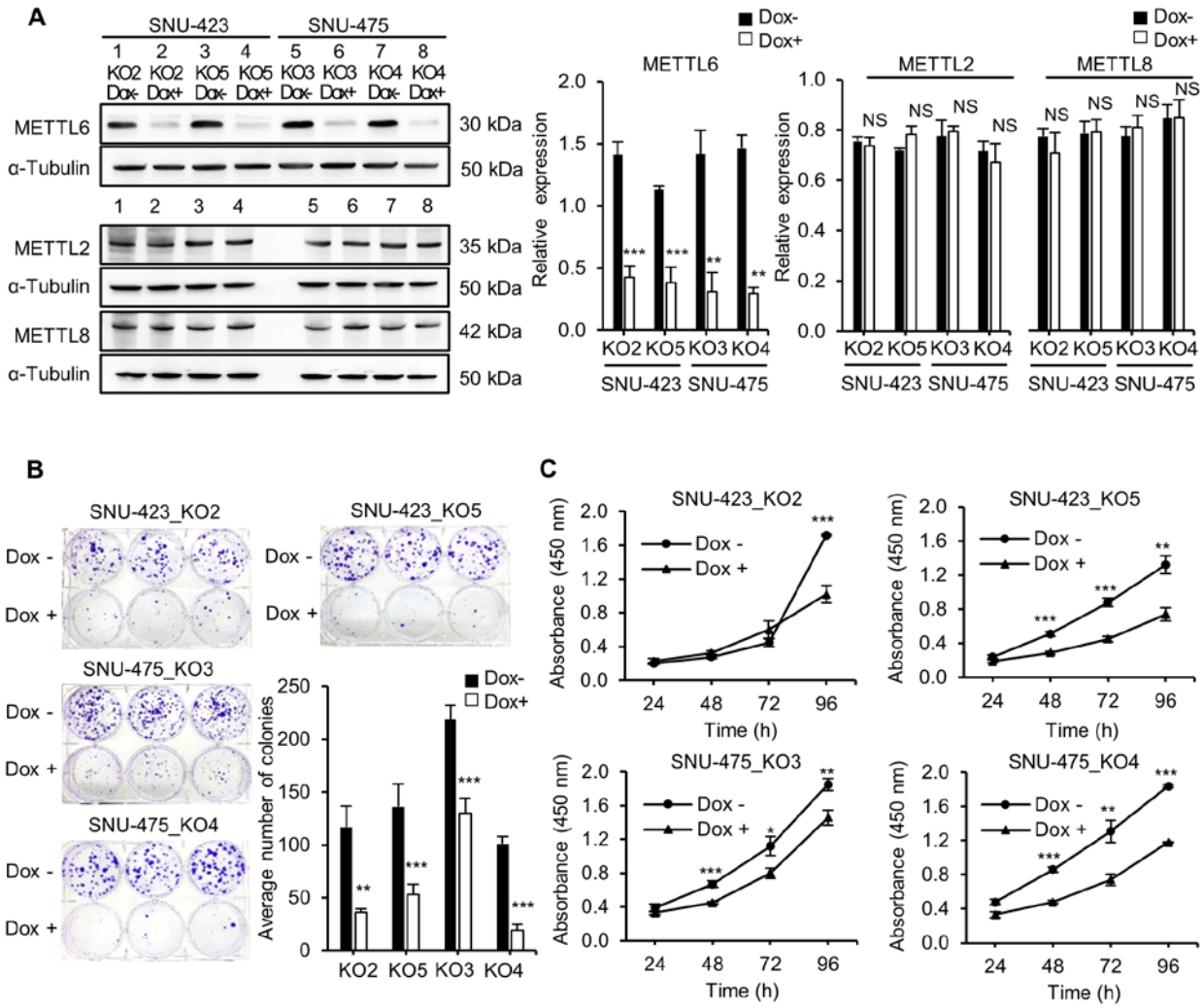

Figure 2. Loss of METTL6 inhibits HCC cell colony formation and proliferation *in vitro*. METTL6 knockout SNU-423 cells and SNU-475 cells were generated by using the CRISPR/Cas9 system with five different guide RNAs and were selected by treatment with doxycycline (Dox+). (A) Western blot analysis of METTL6 protein expression level in SNU-423 and SNU-475 cells with (Dox+) and without (Dox-) Dox treatment. (B) Colony formation assays were conducted to determine the effect of METTL6 on colony formation in the infected HCC cells. Representative images are shown and quantified by ImageJ. (C) Cell proliferation assays are performed to determine the cell viability of infected HCC cells by using the CCK-8 kit. All data are presented as mean ± standard deviation of the least three independent experiments. *P<0.05; **P<0.01; ***P<0.001; NS, non-significant; METTL6, methyltransferase-like 6; HCC, hepatocellular carcinoma.

Loss of METTL6 decreases cell adhesion-related gene expression levels. To investigate the molecular mechanisms of METTL6 action in HCC, we performed RNA-seq on four METTL6 stable knockout cells (SNU-423_KO2, SNU-423_KO5, SNU-475_KO3, and SNU-475_KO4). A heat map and dendrogram summary of the RNA-seq data are shown in Fig. 4A. In total, we identified 1,365 and 1,309 DEGs in SNU-423 and SNU-475 cells, respectively (Fig. 4B). GO analysis using Metascape highlighted that these DEGs were involved in cell-cell adhesion via plasma-membrane adhesion molecules, extracellular matrix, cell migration and invasion, cell apoptotic process, xenobiotic metabolism, and other metabolic processes (Fig. 4C). This indicates that METTL6 may play an important role in cancer cell biology. In addition, there was an overlap of 32 upregulated and 51 downregulated genes between SNU-423 and SNU-475 cells in the different knockout groups (Fig. 4B). Among the downregulated genes, we selected a group of cell adhesion proteins for further investigation, including integrin α-1/β-1 (ITGA1), claudin-14 molecules (CLDN14), and spondin1 (SPON1). ITGA1 mediates the distinct interactions between cells and those in the surrounding extracellular matrix (35); CLDN14 forms tight junctions and interacts with other CAMs (36) while SPON1 is another cell adhesion protein that maintains the extracellular matrix (37). In addition, these cell adhesion genes have been associated with tumor progression and metastasis in HCC (38-40). Immunoblotting revealed that the knockout of METTL6 resulted in a decrease in ITGA1 in SNU-423 cell lines and CLDN14 in SNU-423 and SNU-475 cell lines (Fig. S2B). Unfortunately, SPON1 protein expression was not detected in either SNU-423 or SNU-475. RNA-seq results showed that the average TPM value of ITGA1 in SNU-475 cell lines was 0.351 while it was 1.61 in SNU-423, which could be one of the reasons why the protein expression was relatively weak in SNU-475 cell lines with non-significant decrease after the knockout of METTL6. In addition, the average TPM value of SPON1 among SNU-423 and SNU-475 cell lines was 0.13, which indicated that gene expression levels of SPON1 were

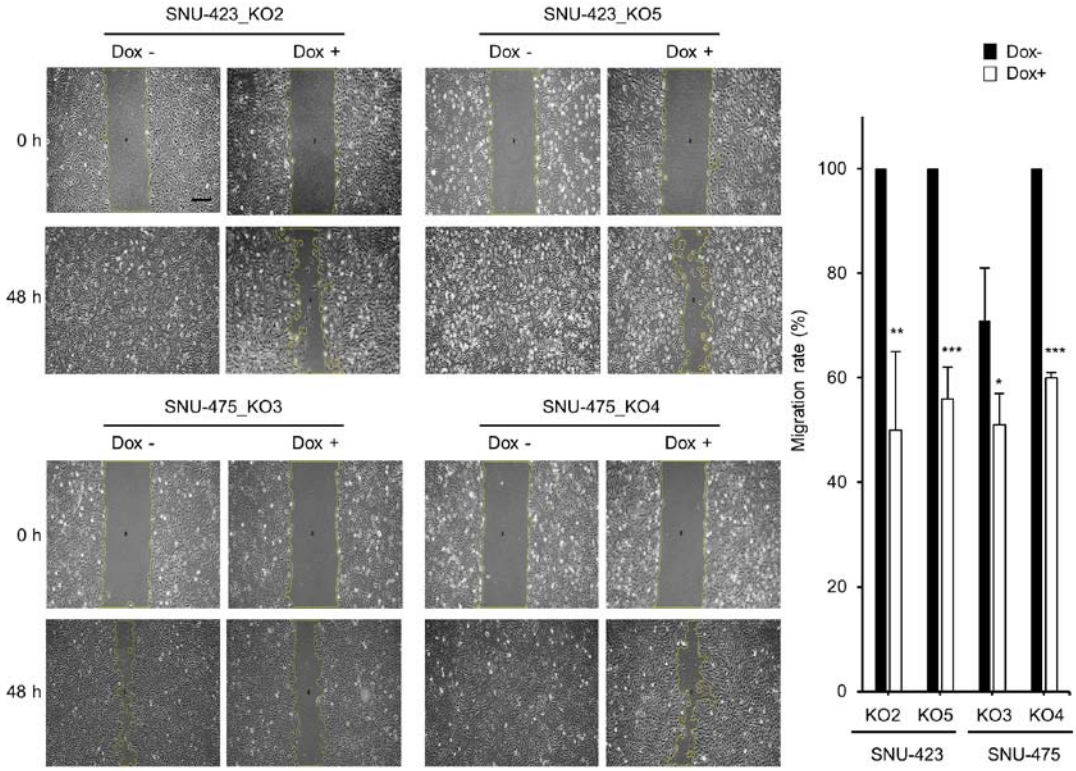

Figure 3. Cell scratch assays determine cell migration of the infected HCC cells. Images are acquired at the start of the experiment (0 h) and 48 h later (48 h) using x4 magnification. Representative images at 0 and 48 h are shown and quantified using ImageJ software. Scale bar, 200 μm. Yellow lines indicate the areas without migrating cells. All data are presented as means ± standard deviation of at least three independent experiments. *P<0.05; **P<0.01; ***P<0.001; NS, non-significant; HCC, hepatocellular carcinoma. Knockout of METTL6 was induced by adding doxycycline (Dox+).

the lowest compared with other proteins. This might explain why SPON1 expression levels were not detected in these cell lines. Our ChIP-seq analysis demonstrated that enhancer activity was not significantly different between control cells and METTL6 KO3 in SNU-475 cells (Fig. S2C). The chromatin binding activity of the transcription factor CTCF also showed a similar binding affinity between the control cells and METTL6 KO3 cell lines (Fig. S2C). These results suggest that METTL6 does not contribute to the transcriptional activity but stabilizes the mRNA expression of cell adhesion genes such as ITGA1 and CLDN14 and increases their protein expression, probably via post-transcriptional tRNA modifications mediated by METTL6.

To determine whether METTL6 depletion attenuated cell adhesion ability and cell invasiveness by altering the expression levels of adhesion molecules, we performed a cell adhesion assay, which is often used to evaluate the metastatic ability of cancer cells. The assay results demonstrated that knockout of METTL6 dramatically decreased the number of attached cells after 60 min in SNU-423 and 45 min in SNU-475 cells (Fig. 5A). Furthermore, we conducted a cell invasion assay and found that the cell invasion ability was significantly suppressed in METTL6 KO cells (Fig. 5B) compared to that in control cells. Taken together, RNA-seq analysis, cell adhesion assay and cell invasion assay results reveal that METTL6 exerts oncogenic effects by altering the expression of CAMs.

METTL6 is localized in the cytoplasm. Our ChIP-seq results suggested that METTL6 was directly associated with post-transcriptional regulation; however, some mRNA expression levels were upregulated and downregulated in METTL6 KO cells. Therefore, we investigated the subcellular localization of METTL6. For this, we conducted immunofluorescence assays and observed an obvious signal reduction in the cytoplasm after the knockout of *METTL6* in SNU-423 and SNU-475 cell lines, indicating that METTL6 was mainly localized in the cytosol (Fig. 6). To the best of our knowledge, this is the first study to confirm that METTL6 is localized in the cytoplasm. In line with our findings, previous studies have shown that METTL6 catalyzes the formation of m^3C at C32 (33,41), and another study claimed that m^3C32 modification must occur in the cytoplasm (42).

Discussion

The field of post-transcriptional regulation of gene expression at the RNA level, and dynamic and reversible modifications of almost all forms of coding and non-coding RNAs, including tRNA, have attracted increasing attention. tRNA is an essential component of protein synthesis. In cancer, deregulation of tRNA can elevate oncogenic protein translation and fulfill the energy demand required for cancerous growth. A recent large-scale analysis revealed an overall overexpression of tRNA levels and amplification of tRNA modification enzymes across 31 cancer types, which indicated the dynamic role of tRNA and tRNA modification proteins in cancer initiation and progression (43). Despite the fact that tRNA modifications are involved in various

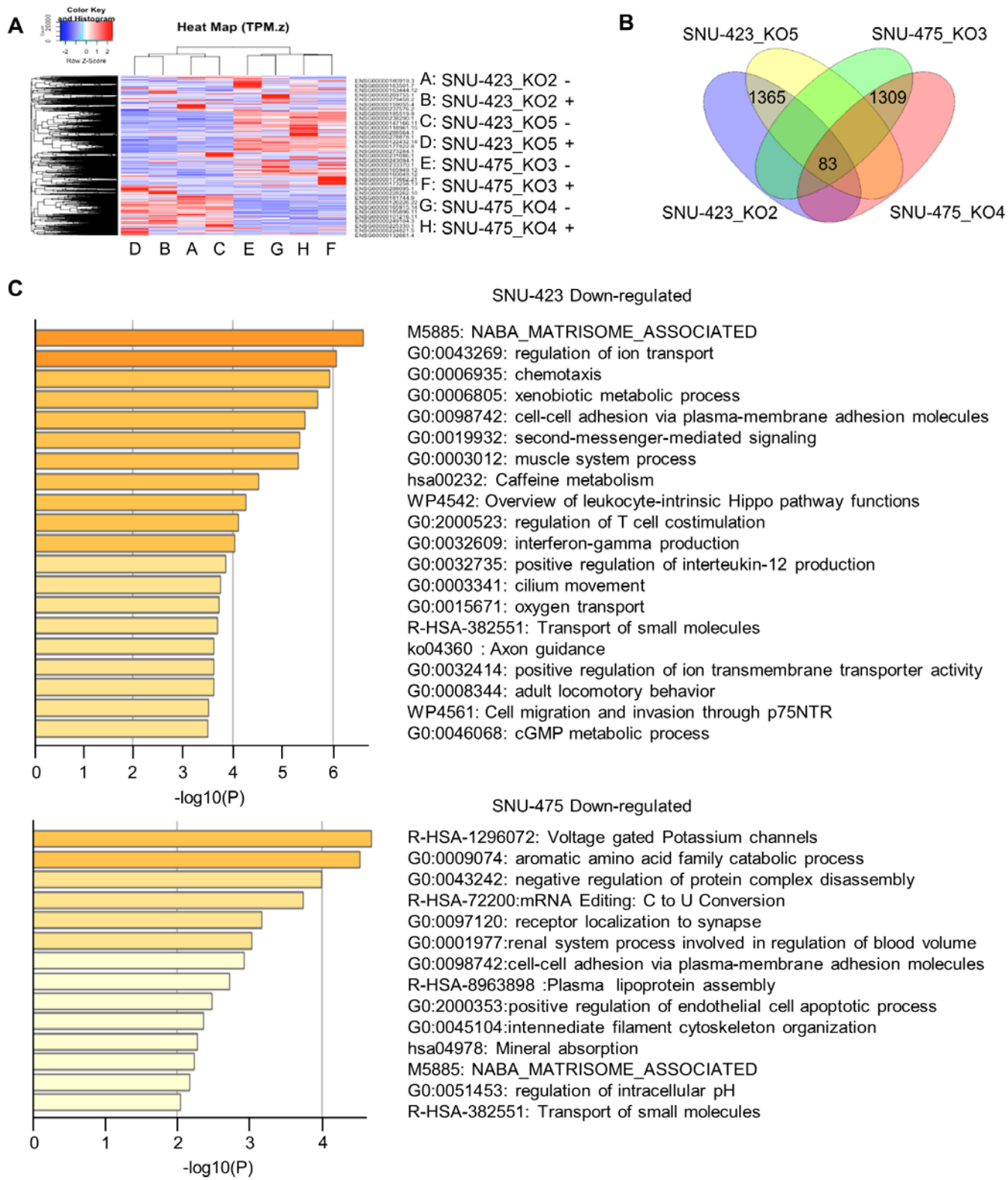

Figure 4. RNA-seq analysis using METTL6 knockout in SNU-423 and SNU-475 cells. (A) Heat Map of RNA-seq results in SNU-423_KO2, SNU-423_KO5, SNU-475_KO3 and SNU-475_KO4 samples. (B) Venn diagram of differentially expressed genes (DEGs) in SNU-423_KO2, SNU-423_KO5, SNU-475_KO3 and SNU-475_KO4 cells. (C) Gene Ontology and Pathway Enrichment Analysis of consistently downregulated genes in two different METTL6 knockouts within SNU-423 cells and SNU-475 cells. METTL6, methyltransferase-like 6.

cancers, the detailed characterization of this process and mechanisms of such regulation are still lacking. This could be attributed to the difficulty of tRNA quantification due to its abundance, and the intricate interactions between tRNA and tumor metabolism (44). METTL6 is a tRNA methylation enzyme that is present in many cancer types; however, we have limited knowledge about its functions and mechanisms of action in cancer. Earlier, the enzymatic activity

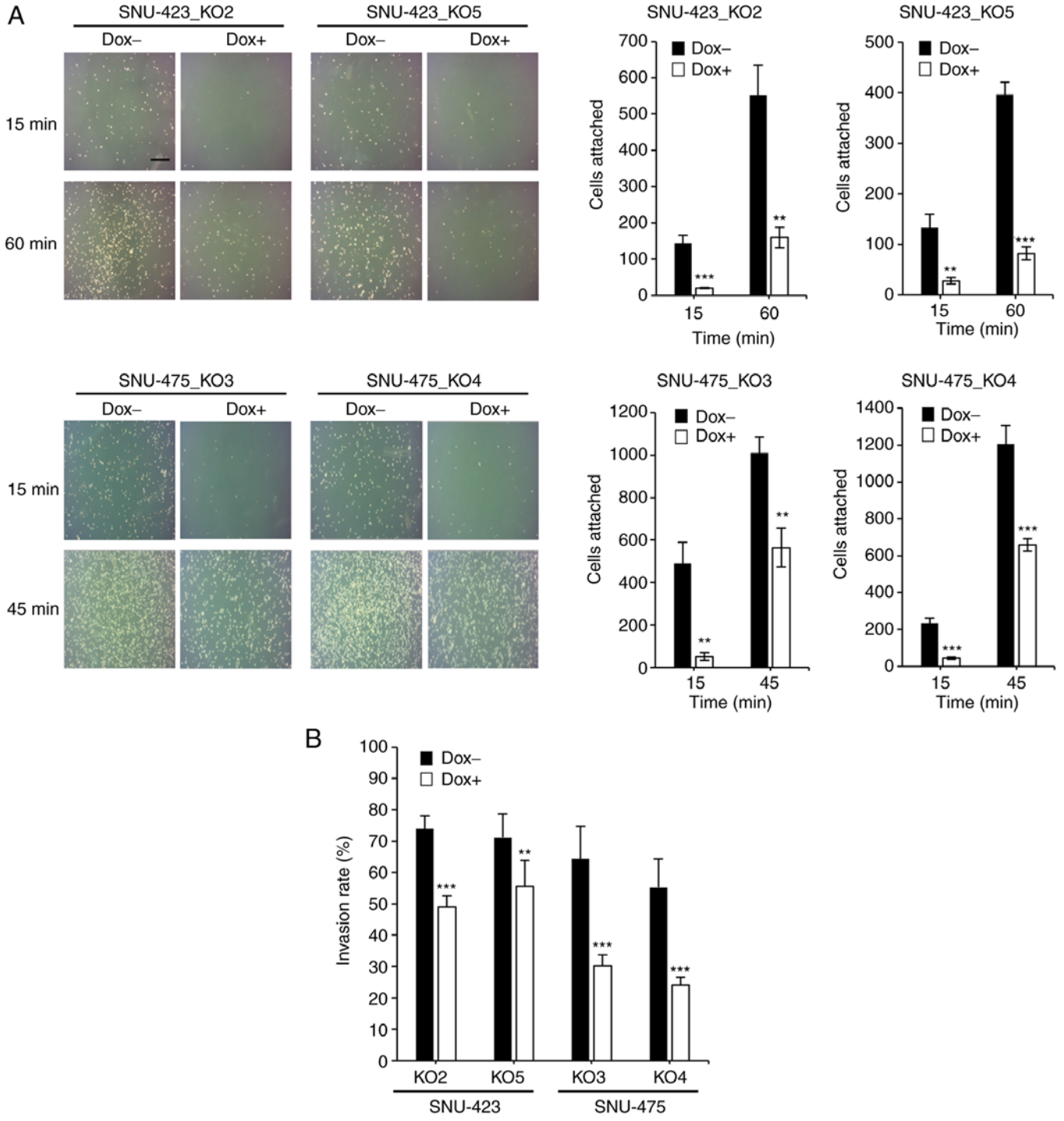

Figure 5. Loss of METTL6 inhibits HCC cell adhesion and cell invasion *in vitro*. (A) Cell adhesion assays were performed to determine the cell adhesion ability of the infected HCC cells. Images are captured at 15, 30, 45, and 60 min after the treated cells were loaded in the culture dishes using x4 magnification. Representative images are shown and quantified using ImageJ software. Scale bar, 200 μm. (B) Cell invasion assays were performed to determine the cell invasiveness of the infected HCC cells. The invasion rate was determined by counting the cells that invaded to the lower chamber compared to the cells added to the top chamber (50,000 cells/well). All data are presented as means ± standard deviation of at least three independent experiments. **P<0.01; ***P<0.001. HCC, hepatocellular carcinoma. METTL6, methyltransferase-like 6; HCC, hepatocellular carcinoma. Knockout of METTL6 was induced by adding doxycycline (Dox+).

of METTL6 was identified by Xu *et al* (33). The knockout of m^3C tRNA-modified enzyme METTL2 showed a 35% reduction, whereas knockout of METTL6 accounted for 12% reduction in the total RNA compared to that in the wild-type (WT) tissues. Moreover, METTL6 is a homolog of Trm141 in *S. pombe*, targeting $tRNA^{Ser}$; therefore, they identified a novel target of tRNA and found that m^3C32 of $tRNA^{Ser(AGA)}$ and $tRNA^{Ser(GCU)}$ were modified by METTL6.

RNA modifications of mRNA are spatiotemporally regulated. For example, METTL14 binds to histone H3 trimethylation at lysine 36 (H3K36me3), and consequently m^6A modification of mRNA is deposited co-transcriptionally (45).

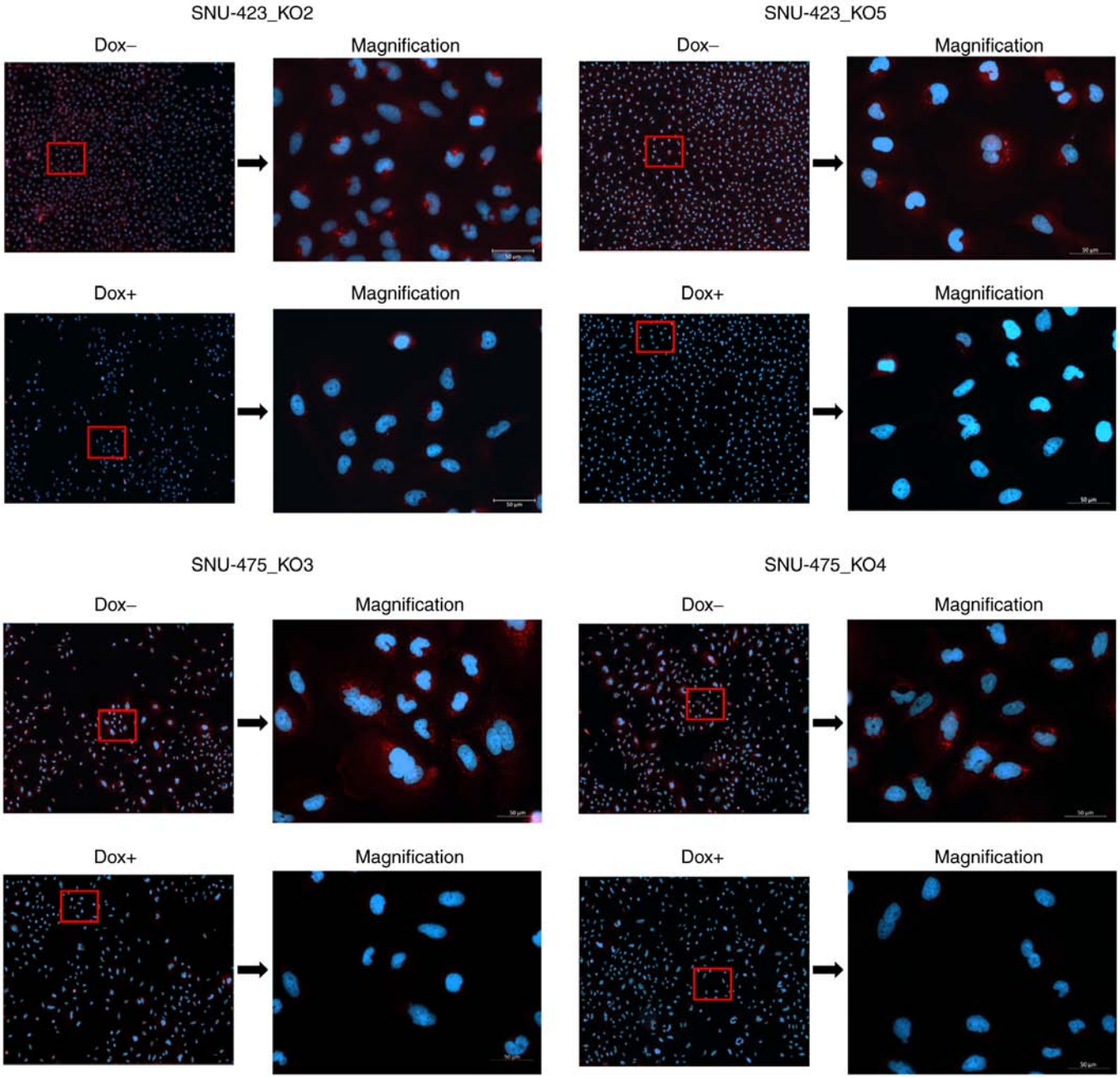

Figure 6. Immunofluorescence experiments demonstrate that METTL6 protein is located in the cytoplasm. Images were captured using x20 magnification. Representative images are shown, which were captured using Celldiscover. Scale bar, 50 μm. METTL6, methyltransferase-like 6. Knockout of METTL6 was induced by adding doxycycline (Dox+).

Intriguingly, the METTL3/METTL14 complex co-transcriptionally regulates histone modification. In the presence of METTL3/METTL14, m^6A modified RNA is recognized by the m^6A reader YTHDC1, which recruits H3K9me2 demethylase KDM3B, and promotes gene expression by demethylating H3K9me2 (46). Similar to m^6A, m^5C and m^5C methyltransferases (RCMTs) contribute to chromatin structure regulation (47). In our data, H3K27ac peak levels were identical between METTL6 expressing and METTL6 depleted cells, suggesting that METTL6 was not associated with transcriptional regulation. This finding was further supported by immunocytochemistry in CRISPR/Cas9-mediated knockout cells, which showed that METTL6 was localized in the cytosol.

As mentioned earlier, more than 170 RNA modifications have been reported, 90 of which are found in tRNAs (1). To date, 14 modification sites have been identified in tRNA (48). It has been reported that modifications of tRNAs affect the stability of tRNAs and thus the genetic code of mRNAs can be read accurately (49). Modifications outside the anticodon region are crucial for tRNA stability and modulating temperature-sensitive growth (50,51). Additional studies have shown that mRNA stability is affected by translation, particularly related to codon stabilization, which is regulated by tRNA anticodon I34 modification by adenosine deaminases (ADATs) (52-54).

The biogenesis and degradation of tRNAs are well summarized by Motorin and Helm (55). Deregulation of early,

intermediate, and late modifications affected tRNA stability and degradation. Destabilization of 3D-structured tRNA triggered by aberrations in RNA modifications involves either the TRAMP pathway (nuclear tRNA degradation) or rapid tRNA decay (cytoplasmic tRNA degradation). Widespread tRNA modification regulates tRNA stability, and hypomodified tRNA is degraded even in bacteria and archaea (56). Therefore, it is reasonable to assume that METTTL6 may regulate tRNA stability in SNU-423 and SNU-475 cell lines and possibly affect mRNA expression levels, followed by alterations in protein expression.

A tRNA half, which binds with other transcripts and regulates gene expression as miRNA, may account for a possible explanation of how METTL6 mediates mRNA expression levels. tRNA halves are generated by dicers, angiogenins, or other exonucleases (57,58). Intriguingly, RNA modifications play important roles in the origin and function of tRNA fragments, and tRNA modifications promote and protect the expression of tRNA halves (59). Moreover, tRNA-derived fragments regulate ribosomal biogenesis by targeting ribosomal proteins encoding two mRNAs in a mouse model of HCC (60).

In the present study, we focused on METTL6 and explored its oncogenic activities in HCC, thereby providing a novel perspective on its underlying mechanism in cancer progression by altering the expression levels of membrane proteins. Here, for the first time, we performed a comprehensive bioinformatics analysis of RNA modification enzymes and associated proteins in patients with HCC using a liver cancer dataset and observed that METTL6 was upregulated in HCC tissues compared to the adjacent non-tumor tissue samples. High expression levels of METTL6 were associated with high histological grade and poor survival rates, suggesting that METTL6 was a potential unfavorable prognostic biomarker in HCC. To further investigate the functional role of METTL6 in HCC, we knocked out *METTL6* through the CRISPR/Cas9 system *in vitro* using five independent gRNAs, and demonstrated that the depletion of METTL6 significantly suppressed HCC cell growth, colony formation, cell migration, cell invasion and cell adhesion. In addition, we used RNA-seq and ChIP-seq to elucidate the mechanism of METTL6-driven regulation of HCC. In addition to GO and pathway enrichment analysis, we found that knockout of METTL6 significantly reduced the expression levels of cell adhesion proteins, including ITGA1, SPON1, and CLDN14, which was further validated at the protein level.

Previous studies have demonstrated that the abovementioned cell adhesion proteins are of crucial importance in HCC and other cancers. Liu *et al* reported that silencing of ITGA1 inhibited HCC cell migration and invasion, while upregulation of ITGA1 enhanced HCC migration and invasion ability *in vitro* (38). In addition, overexpression of ITGA1 has been indicated as a key driver of HCC lymph gland metastasis (61). Gharibi *et al* found that ITGA was increased in pancreatic cancer and associated with poor prognosis, and that ITGA1 was necessary for TGFβ/collagen-induced epithelial to mesenchymal transition and metastasis (62). Another study suggested that ITGA1 could promote colorectal cancer cell migration, invasion, and tumorigenicity by activating Ras/Erk signaling (63). Interestingly, our RNA-seq results also showed a significant decrease in the activity of the Ras signaling pathway along with ITGA1, such as T-cell lymphoma invasion and metastasis-inducing protein 1 (TIAM1) and GRB2-associated-binding protein 2 (GAB2), while there was an increase in the expression of kinase suppressor of Ras 2 (KSR2), which is a Ras/Erk signaling suppressor, after the knockout of METTL6. Dai *et al* demonstrated that downregulation of SPON1 inhibited HCC cell proliferation, migration, and invasion (39). Of note, high *CLDN14* expression was associated with good prognosis in HCC (P=0.047) analyzed using GEPIA. However, there are some contradictory findings regarding the prognostic role of CLDN14 in cancer. One study showed that CLDN14 was a favorable prognostic biomarker in HCC (40), and that CLDN14 was a direct target of EZH2-mediated H3K27me3 and regulated by the Wnt/β-catenin pathway (40). RNA-seq analysis in our study indicated that *EZH2* expression was not altered. The expression levels of Wnt family proteins (2B, 3, 5A, 5B, 6, 7B, 10A, and 10B) were altered (downregulated, no difference, and upregulated). Tryndyak *et al* reported that cytosine DNA hypermethylation induced the downregulation of *CLDN14* gene expression in differentiated HepaRG cells treated with $NaAsO_2$ (64). Another study revealed that the *CLDN14* expression level was negatively correlated with acute myeloid leukemia (AML) survival rates (65). In breast cancer (BC), *CLDN14* gene expression was upregulated in BC tissues compared with non-cancer tissues, and a high gene expression of *CLDN14* was associated with a poor overall survival (66). These previous reports suggest that *CLDN14* gene expression, as well as the relationship between gene expression and patient outcome, are dependent on various cellular contexts.

The primary challenges of focusing on METTL6 or tRNA modifications are the lack of m^3C recognizing antibody for RNA immunoprecipitation sequencing to globally address specific m^3C tRNA modification as well as the lack of established tRNA-focused next-generation sequencing techniques, which means that solid analyzing pipelines are currently missing. Hence, we need to continue developing biochemical analytical tools and delve further into this field for a comprehensive understanding of the role of tRNA modifications.

One limitation of our study is the difficulty in revealing how METTL6 interacts with identified cell adhesion proteins and regulates their role in cancer cell proliferation, migration, invasion and adhesion. Therefore, further detailed research and validation such as rescue experiments are required. The other option is to perform pulldown experiments to pulldown m^3C modified RNA and conduct a high-throughput analysis (known as MeRIP-seq; methylated RNA immunoprecipitation) to detect m^3C modified tRNA using METTL6-expressing cells (Dox-) and METTL6-KO cells (Dox+). This may provide a more direct indication of whether global or specific tRNA modifications by METTL6 are associated with target gene expression. For validation, control tRNAs and mutant tRNAs at methylated positions should be transfected and confirmed by experimentally changing the expression levels of the methylated tRNAs. In addition, it is needed to conduct mass spectrometry analysis in advance to determine the precise methylated position on the RNAs of interest. However, there are some technical concerns such as the lack of antibodies to recognize m^3C (specificity, sensitivity, and precipitation efficacy), and/or MeRIP platform for tRNA. Another limitation of current

study is that we only investigated the role of METTL6 in HCC using cell lines, but did not verify our findings *in vivo*. The xenograft mouse models will be established in future studies to support the findings of the present study.

Acknowledgements

The authors express their gratitude to the past and present members of the Hamamoto Laboratory. AB is grateful to the Otsuka Toshimi Scholarship Foundation for their support during her PhD study.

Funding

This study was supported by JST CREST (grant no. JPMJCR1689), JSPS Grant-in-Aid for Scientific Research on Innovative Areas (grant no. JP18H04908), and JSPS KAKENHI (grant no. JP20K17982).

Availability of data and materials

The datasets used and/or analyzed in the present study are available from the corresponding author upon reasonable request.

Authors' contributions

AB, KA, SK, and RH designed the study. AB, KA, SK, KS, and NI performed the experiments. AB, KA, SK, and HM analyzed the data and confirmed the accuracy. AB and KA wrote the manuscript. MK, SS, and RH reviewed, edited, revised critically and proposed feedback constructive suggestions to improve the quality of the manuscript. All authors read and approved the manuscript and agree to be accountable for all aspects of the research in ensuring that the accuracy or integrity of any part of the work are appropriately investigated and resolved.

Ethics approval and consent to participate

Not applicable.

Patient consent for publication

Not applicable.

Competing interests

The authors declare that they have no competing interests.

References

1. Boccaletto P, Machnicka MA, Purta E, Piatkowski P, Baginski B, Wirecki TK, de Crécy-Lagard V, Ross R, Limbach PA, Kotter A, *et al*: MODOMICS: A database of RNA modification pathways. 2017 update. Nucleic Acids Res 46: D303-D307, 2018.
2. Barbieri I and Kouzarides T: Role of RNA modifications in cancer. Nat Rev Cancer 20: 303-322, 2020.
3. Delaunay S and Frye M: RNA modifications regulating cell fate in cancer. Nat Cell Biol 21: 552-559, 2019.
4. Roundtree IA, Evans ME, Pan T and He C: Dynamic RNA modifications in gene expression regulation. Cell 169: 1187-1200, 2017.
5. Asada K, Bolatkan A, Takasawa K, Komatsu M, Kaneko S and Hamamoto R: Critical Roles of N^6-Methyladenosine (m^6A) in cancer and virus infection. Biomolecules 10: 1071, 2020.
6. Bray F, Ferlay J, Soerjomataram I, Siegel RL, Torre LA and Jemal A: Global cancer statistics 2018: GLOBOCAN estimates of incidence and mortality worldwide for 36 cancers in 185 countries. CA Cancer J Clin 68: 394-424, 2018.
7. Herath NI, Leggett BA and MacDonald GA: Review of genetic and epigenetic alterations in hepatocarcinogenesis. J Gastroenterol Hepatol 21: 15-21, 2006.
8. Nishida N and Goel A: Genetic and epigenetic signatures in human hepatocellular carcinoma: A systematic review. Curr Genomics 12: 130-137, 2011.
9. Hamamoto R, Furukawa Y, Morita M, Iimura Y, Silva FP, Li M, Yagyu R and Nakamura Y: SMYD3 encodes a histone methyltransferase involved in the proliferation of cancer cells. Nat Cell Biol 6: 731-740, 2004.
10. Yagyu R, Hamamoto R, Furukawa Y, Okabe H, Yamamura T and Nakamura Y: Isolation and characterization of a novel human gene, VANGL1, as a therapeutic target for hepatocellular carcinoma. Int J Oncol 20: 1173-1178, 2002.
11. Shigekawa Y, Hayami S, Ueno M, Miyamoto A, Suzaki N, Kawai M, Hirono S, Okada KI, Hamamoto R and Yamaue H: Overexpression of KDM5B/JARID1B is associated with poor prognosis in hepatocellular carcinoma. Oncotarget 9: 34320-34335, 2018.
12. Ryu JW, Kim SK, Son MY, Jeon SJ, Oh JH, Lim JH, Cho S, Jung CR, Hamamoto R, Kim DS and Cho HS: Novel prognostic marker PRMT1 regulates cell growth via downregulation of CDKN1A in HCC. Oncotarget 8: 115444-115455, 2017.
13. Chen M, Wei L, Law CT, Tsang FH, Shen J, Cheng CL, Tsang LH, Ho DW, Chiu DK, Lee JM, *et al*: RNA N6-methyladenosine methyltransferase-like 3 promotes liver cancer progression through YTHDF2-dependent posttranscriptional silencing of SOCS2. Hepatology 67: 2254-2270, 2018.
14. Barbieri I, Tzelepis K, Pandolfini L, Shi J, Millán-Zambrano G, Robson SC, Aspris D, Migliori V, Bannister AJ, Han N, *et al*: Promoter-bound METTL3 maintains myeloid leukaemia by m^6A-dependent translation control. Nature 552: 126-131, 2017.
15. Ma JZ, Yang F, Zhou CC, Liu F, Yuan JH, Wang F, Wang TT, Xu QG, Zhou WP and Sun SH: METTL14 suppresses the metastatic potential of hepatocellular carcinoma by modulating N^6-methyladenosine-dependent primary MicroRNA processing. Hepatology 65: 529-543, 2017.
16. Bao J, Yu Y, Chen J, He Y, Chen X, Ren Z, Xue C, Liu L, Hu Q, Li J, *et al*: MiR-126 negatively regulates PLK-4 to impact the development of hepatocellular carcinoma via ATR/CHEK1 pathway. Cell Death Dis 9: 1045, 2018.
17. Zhong L, Liao D, Zhang M, Zeng C, Li X, Zhang R, Ma H and Kang T: YTHDF2 suppresses cell proliferation and growth via destabilizing the EGFR mRNA in hepatocellular carcinoma. Cancer Lett 442: 252-261, 2019.
18. Gatza ML, Silva GO, Parker JS, Fan C and Perou CM: An integrated genomics approach identifies drivers of proliferation in luminal-subtype human breast cancer. Nat Genet 46: 1051-1059, 2014.
19. Tan XL, Moyer AM, Fridley BL, Schaid DJ, Niu N, Batzler AJ, Jenkins GD, Abo RP, Li L, Cunningham JM, *et al*: Genetic variation predicting cisplatin cytotoxicity associated with overall survival in lung cancer patients receiving platinum-based chemotherapy. Clin Cancer Res 17: 5801-5811, 2011.
20. Ignatova VV, Kaiser S, Ho JS, Bing X, Stolz P, Tan YX, Lee CL, Gay FP, Lastres PR, Gerlini R, *et al*: METTL6 is a tRNA m^3C methyltransferase that regulates pluripotency and tumor cell growth. Sci Adv 6: eaaz4551, 2020.
21. Dai X, Jiang W, Ma L, Sun J, Yan X, Qian J, Wang Y, Shi Y, Ni S and Yao N: A metabolism-related gene signature for predicting the prognosis and therapeutic responses in patients with hepatocellular carcinoma. Ann Transl Med 9: 500, 2021.
22. Lopez-Terrada D, Cheung SW, Finegold MJ and Knowles BB: Hep G2 is a hepatoblastoma-derived cell line. Hum Pathol 40: 1512-1515, 2009.
23. Nakabayashi H and Taketa K: HuH-7 cell line established from a highly differentiated human hepatocellular carcinoma. Okayama Igakkai Zasshi (Journal of Okayama Medical Association) 124: 231-238, 2012.
24. Yamada T, Abei M, Danjoh I, Shirota R, Yamashita T, Hyodo I and Nakamura Y: Identification of a unique hepatocellular carcinoma line, Li-7, with CD13(+) cancer stem cells hierarchy and population change upon its differentiation during culture and effects of sorafenib. BMC Cancer 15: 260, 2015.

25. Kim S, Bolatkan A, Kaneko S, Ikawa N, Asada K, Komatsu M, Hayami S, Ojima H, Abe N, Yamaue H and Hamamoto R: Deregulation of the histone lysine-specific demethylase 1 is involved in human hepatocellular carcinoma. Biomolecules 9: 810, 2019.
26. Schneider CA, Rasband WS and Eliceiri KW: NIH Image to ImageJ: 25 years of image analysis. Nat Methods 9: 671-675, 2012.
27. Zhou Y, Zhou B, Pache L, Chang M, Khodabakhshi AH, Tanaseichuk O, Benner C and Chanda SK: Metascape provides a biologist-oriented resource for the analysis of systems-level datasets. Nat Commun 10: 1523, 2019.
28. Ozawa T, Kaneko S, Szulzewsky F, Qiao Z, Takadera M, Narita Y, Kondo T, Holland EC, Hamamoto R and Ichimura K: C11orf95-RELA fusion drives aberrant gene expression through the unique epigenetic regulation for ependymoma formation. Acta Neuropathol Commun 9: 36, 2021.
29. Langmead B and Salzberg SL: Fast gapped-read alignment with Bowtie 2. Nat Methods 9: 357-359, 2012.
30. Robinson JT, Thorvaldsdottir H, Winckler W, Guttman M, Lander ES, Getz G and Mesirov JP: Integrative genomics viewer. Nat Biotechnol 29: 24-26, 2011.
31. Tang Z, Li C, Kang B, Gao G, Li C and Zhang Z: GEPIA: A web server for cancer and normal gene expression profiling and interactive analyses. Nucleic Acids Res 45: W98-W102, 2017.
32. Anaya J: OncoLnc: Linking TCGA survival data to mRNAs, miRNAs, and lncRNAs. PeerJ Computer Science 2: e67, 2016.
33. Xu L, Liu X, Sheng N, Oo KS, Liang J, Chionh YH, Xu J, Ye F, Gao YG, Dedon PC and Fu XY: Three distinct 3-methylcytidine (m^3C) methyltransferases modify tRNA and mRNA in mice and humans. J Biol Chem 292: 14695-14703, 2017.
34. Richon VM, Johnston D, Sneeringer CJ, Jin L, Majer CR, Elliston K, Jerva LF, Scott MP and Copeland RA: Chemogenetic analysis of human protein methyltransferases. Chem Biol Drug Des 78: 199-210, 2011.
35. Leitinger B and Hohenester E: Mammalian collagen receptors. Matrix Biol 26: 146-155, 2007.
36. Wilcox ER, Burton QL, Naz S, Riazuddin S, Smith TN, Ploplis B, Belyantseva I, Ben-Yosef T, Liburd NA, Morell RJ, *et al*: Mutations in the gene encoding tight junction claudin-14 cause autosomal recessive deafness DFNB29. Cell 104: 165-172, 2001.
37. Klar A, Baldassare M and Jessell TM: F-spondin: A gene expressed at high levels in the floor plate encodes a secreted protein that promotes neural cell adhesion and neurite extension. Cell 69: 95-110, 1992.
38. Liu X, Tian H, Li H, Ge C, Zhao F, Yao M and Li J: Derivate Isocorydine (d-ICD) suppresses migration and invasion of hepatocellular carcinoma cell by downregulating ITGA1 expression. Int J Mol Sci 18: 514, 2017.
39. Dai W, Huang HL, Hu M, Wang SJ, He HJ, Chen NP and Li MY: microRNA-506 regulates proliferation, migration and invasion in hepatocellular carcinoma by targeting F-spondin 1 (SPON1). Am J Cancer Res 5: 2697-2707, 2015.
40. Li CP, Cai MY, Jiang LJ, Mai SJ, Chen JW, Wang FW, Liao YJ, Chen WH, Jin XH, Pei XQ, *et al*: CLDN14 is epigenetically silenced by EZH2-mediated H3K27ME3 and is a novel prognostic biomarker in hepatocellular carcinoma. Carcinogenesis 37: 557-566, 2016.
41. Arimbasseri AG, Iben J, Wei FY, Rijal K, Tomizawa K, Hafner M and Maraia RJ: Evolving specificity of tRNA 3-methyl-cytidine-32 (m3C32) modification: A subset of tRNAsSer requires N6-isopentenylation of A37. RNA 22: 1400-1410, 2016.
42. Hopper AK and Huang HY: Quality control pathways for nucleus-encoded eukaryotic tRNA biosynthesis and subcellular trafficking. Mol Cell Biol 35: 2052-2058, 2015.
43. Zhang Z, Ye Y, Gong J, Ruan H, Liu CJ, Xiang Y, Cai C, Guo AY, Ling J and Diao L: Global analysis of tRNA and translation factor expression reveals a dynamic landscape of translational regulation in human cancers. Commun Biol 1: 234, 2018.
44. Santos M, Fidalgo A, Varanda AS, Oliveira C and Santos MA: tRNA deregulation and its consequences in cancer. Trends Mol Med 25: 853-865, 2019.
45. Huang H, Weng H, Zhou K, Wu T, Zhao BS, Sun M, Chen Z, Deng X, Xiao G, Auer F, *et al*: Histone H3 trimethylation at lysine 36 guides m^6A RNA modification co-transcriptionally. Nature 567: 414-419, 2019.
46. Li Y, Xia L, Tan K, Ye X, Zuo Z, Li M, Xiao R, Wang Z, Liu X, Deng M, *et al*: N^6-Methyladenosine co-transcriptionally directs the demethylation of histone H3K9me2. Nat Genet 52: 870-877, 2020.
47. Cheng JX, Chen L, Li Y, Cloe A, Yue M, Wei J, Watanabe KA, Shammo JM, Anastasi J, Shen QJ, *et al*: RNA cytosine methylation and methyltransferases mediate chromatin organization and 5-azacytidine response and resistance in leukaemia. Nat Commun 9: 1163, 2018.
48. Pereira M, Francisco S, Varanda AS, Santos M, Santos MA and Soares AR: Impact of tRNA Modifications and tRNA-modifying enzymes on proteostasis and human disease. Int J Mol Sci 19: 3738, 2018.
49. Hoffer ED, Hong S, Sunita S, Maehigashi T, Gonzalez RL Jnr, Whitford PC and Dunham CM: Structural insights into mRNA reading frame regulation by tRNA modification and slippery codon-anticodon pairing. Elife 9: e51898, 2020.
50. McLaughlin CS, Grundberg-Manago M, Dondon J, Michelson AM and Saunders G: Stability of the messenger RNA-transfer RNA-ribosome complex. J Mol Biol 32: 521-542, 1968.
51. Alexandrov A, Chernyakov I, Gu W, Hiley SL, Hughes TR, Grayhack EJ and Phizicky EM: Rapid tRNA decay can result from lack of nonessential modifications. Mol Cell 21: 87-96, 2006.
52. Carneiro RL, Requiao RD, Rossetto S, Domitrovic T and Palhano FL: Codon stabilization coefficient as a metric to gain insights into mRNA stability and codon bias and their relationships with translation. Nucleic Acids Res 47: 2216-2228, 2019.
53. Wu Q, Medina SG, Kushawah G, DeVore ML, Castellano LA, Hand JM, Wright M and Bazzini AA: Translation affects mRNA stability in a codon-dependent manner in human cells. Elife 8: e45396, 2019.
54. Lyu X, Yang Q, Li L, Dang Y, Zhou Z, Chen S and Liu Y: Adaptation of codon usage to tRNA I34 modification controls translation kinetics and proteome landscape. PLoS Genet 16: e1008836, 2020.
55. Motorin Y and Helm M: tRNA stabilization by modified nucleotides. Biochemistry 49: 4934-4944, 2010.
56. Kimura S and Waldor MK: The RNA degradosome promotes tRNA quality control through clearance of hypomodified tRNA. Proc Natl Acad Sci USA 116: 1394-1403, 2019.
57. Schimmel P: The emerging complexity of the tRNA world: Mammalian tRNAs beyond protein synthesis. Nat Rev Mol Cell Biol 19: 45-58, 2018.
58. Xie Y, Yao L, Yu X, Ruan Y, Li Z and Guo J: Action mechanisms and research methods of tRNA-derived small RNAs. Signal Transduct Target Ther 5: 109, 2020.
59. Lyons SM, Fay MM and Ivanov P: The role of RNA modifications in the regulation of tRNA cleavage. FEBS Lett 592: 2828-2844, 2018.
60. Kim HK, Fuchs G, Wang S, Wei W, Zhang Y, Park H, Roy-Chaudhuri B, Li P, Xu J, Chu K, *et al*: A transfer-RNA-derived small RNA regulates ribosome biogenesis. Nature 552: 57-62, 2017.
61. Wan J, Wen D, Dong L, Tang J, Liu D, Liu Y, Tao Z, Gao D, Sun H, Cao Y, *et al*: Establishment of monoclonal HCC cell lines with organ site-specific tropisms. BMC Cancer 15: 678, 2015.
62. Gharibi A, La Kim S, Molnar J, Brambilla D, Adamian Y, Hoover M, Hong J, Lin J, Wolfenden L and Kelber JA: ITGA1 is a pre-malignant biomarker that promotes therapy resistance and metastatic potential in pancreatic cancer. Sci Rep 7: 10060, 2017.
63. Li H, Wang Y, Rong SK, Li L, Chen T, Fan YY, Wang YF, Yang CR, Yang C, Cho WC and Yang J: Integrin α1 promotes tumorigenicity and progressive capacity of colorectal cancer. Int J Biol Sci 16: 815-826, 2020.
64. Tryndyak VP, Borowa-Mazgaj B, Steward CR, Beland FA and Pogribny IP: Epigenetic effects of low-level sodium arsenite exposure on human liver HepaRG cells. Arch Toxicol 94: 3993-4005, 2020.
65. Cheng J, Han J and Lin C: A comprehensive assessment of the prognostic role of cell adhesion molecules in acute myeloid leukemia. Transl Cancer Res 9: 7605-7618, 2020.
66. Yang G, Jian L and Chen Q: Comprehensive analysis of expression and prognostic value of the claudin family in human breast cancer. Aging (Albany NY) 13: 8777-8796, 2021.